Fiber and Integrated Optics, Volume 13, pp. 165–183
Printed in the UK.

0146-8030/94 $10.00 + .00

Architectures and Techniques for All-Optical Networks

FABRIZIO FORGHIERI

Dipartimento di Ingegneria dell'Informazione
Università di Parma
Viale delle Scienze
Parma, Italy

ALBERTO BONONI

Department of Electrical Engineering
Princeton University
Princeton, New Jersey, USA

JIAN-GUO ZHANG

Dipartimento di Ingegneria dell'Informazione
Università di Parma
Viale delle Scienze
Parma, Italy

PAUL R. PRUCNAL

Department of Electrical Engineering
Princeton University
Princeton, New Jersey, USA

GIORGIO PICCHI AND GIANCARLO PRATI

Dipartimento di Ingegneria dell'Informazione
Università di Parma
Viale delle Scienze
Parma, Italy

Some recent results on all-optical packet-switching and broadcasting networks are presented. The performance evaluation problem of packet-switching transparent optical networks with deflection routing is addressed. Transmission error arguments show how, for a given optical bit rate, the size of an all-optical nonregenerative multihop network is limited by the accumulation of noise and distortion in the optical fiber channel. Time-domain multiple access techniques are exploited in novel

Received 20 July 1993; accepted 4 August 1993.
A. Bononi is on leave from Dipartimento di Ingegneria dell'Informazione, Università di Parma.
Address correspondence to F. Forghieri, Dipartimento di Ingegneria dell'Informazione, Università di Parma, Viale delle Scienze, I-43100, Parma, Italy.

architectures based on recently proposed all-optical sampling gates to realize the matching of the ultrahigh optical speed allowed by the large bandwidth of the fiber with the lower speed of the electronic components needed at the user ends. These architectures allow great simplification of the node structure in the considered all-optical multihop and broadcast networks.

Optical fibers are rapidly superseding copper cables at all levels of local-, metropolitan-, and wide-area data networks. The same is happening in telephone networks at the trunk level, and fibers are also being considered for use in the tomorrow's subscriber loop.

However, the deployment of optical fibers has not produced any real revolution in design, architecture, and performance of telecommunication networks as it could be expected by the wide use of a medium that in many aspects is revolutionary. The reason for this is that fibers have been introduced mainly as small, low-attenuation, and low-cost *substitutes* of copper cables in the existing networks. So doing, the really revolutionary feature of fibers, bandwidth, has not been exploited. This was partially due to the operating speed of opto-electronic components that has never been capable of operating at speeds comparable to the fiber's bandwidth.

In fact, the only way to exploit fully the extraordinary fiber's bandwidth is to create a large-bandwidth optical signal by multiplexing at the optical level a large number of signals capable of being individually processed at the electronic level. Once generated, the multiplexed signal shall never be converted to the electrical domain at any points of its propagation path. Dropping and inserting users is possible because only one channel at a time is processed by the electro-optical interfaces.

Optical networks based on these principles are called all-optical or transparent networks and are the subjects of active research in many laboratories and universities in the world. The common goal is the demonstration that optical networks operating at speeds in the range of hundreds of gigabits per second are a technical possibility. To achieve this performance most of the processing, like multiplexing, demultiplexing, and switching, must be performed at the optical level.

As part of their research work the authors present here some recent results on all-optical packet-switching and broadcast networks. Part of this work stems from the cooperation between Parma University, Italy, and Princeton University, USA.

The next section introduces the performance evaluation problem of packet-switching transparent optical networks with deflection routing, considering the effects of the optical channel. The third section presents a simple single-buffer deflection routing technique, whose effectiveness is analytically evaluated in uniform traffic and compared to the case of no buffers (hot-potato) and infinite buffers (ideal store-and-forward). Section four gives the structure of the optical node, where new techniques to reduce the implementation complexity are introduced. The fifth section presents the results of a theoretical packet error rate analysis in two-connected Manhattan Street and ShuffleNet networks when on–off soliton packet transmission is used at a fixed optical wavelength and at bit rates in the 100 Gb/s range. Section six presents a novel technique for bit synchronization in a time division multiple access (TDMA) broadcast network. The final section describes an extension of synchronous TDMA networks to the case of multirate data communications.

Packet-Switching Transparent Optical Networks

Ultrahigh bit rates may be used in packet-switching transparent optical networks since the transmitted signal remains in optical form from source to destination and electronic conversions occur only at the end points of the connection. An all-optical, transparent pipe is dynamically allocated between the end users.

At ultrahigh rates, the complexity of the routing and switching processes in the network has to be kept as low as possible. Distributed mesh topologies break down this computational complexity by evenly sharing this burden, which increases exponentially with the number of users, among all nodes. In two-connected networks, for instance, each node has only two optical inputs and two optical outputs, and the local routing and switching problem is thus reduced to a binary decision on the state of the switch. Very simple minimum-distance routing algorithms have been found for networks with regular topology, such as Manhattan Street (MS) [1] and ShuffleNet (SN) [2].

Research toward a simpler control of the switching process produced the deflection routing algorithm [3, 4]. This proved to be even more attractive in transparent optical networks, where one of the technological limitations is the lack of very fast access, flexible, simple optical memories. The limited-time buffering strategy of deflection routing is perfectly suited to be implemented with simple recirculating fiber delay loops, with no need of optical amplification in the loop.

Both multihop distributed networks (as opposed to single-hop, centralized networks) and deflection routing (as opposed to store-and-forward (S&F) routing) are solutions that trade efficiency for a much simpler hardware implementation and enhanced reliability. If ultrahigh bit rates can be sustained by these distributed structures using deflection routing, then a net gain in throughput can effectively be achieved [5].

Extremely simple system solutions must be used in the design of the nodes in these transparent networks to minimize the complexity of the optical components in order to reduce the flow-through optical power loss per node and to lower the complexity of the electronic processing in the routing block.

The bandwidth mismatch between the electronic interfaces at the end users and the optical pipe can be overcome by parallelizing the electronics. Recently proposed all-optical sampling techniques may be used to demodulate packets at bit rates far beyond the speed of conventional optical receivers.

However, transparency implies that no regeneration of the optical packets is provided at intermediate nodes. Noise and distortion in the optical fiber channel accumulate as the packets propagate so that the physical distance from source to destination is constrained at a given optical bit rate if the packet error rate is to be bounded below a given threshold. Repeatedly deflected packets travel long distances before reaching their destination and are thus more likely to be in error at the receiver. Due to the randomness of the routing technique, the packet error rate can be obtained by conditioning on the random number of hops n taken by a typical packet to reach its destination in a regular multihop network with equal link lengths as

$$\mathrm{P}(e) = \sum_{n=1}^{\infty} \mathrm{P}(e/n)\mathrm{P}(n) \tag{1}$$

The average hop distribution P(n) depends only on network topology, routing, and load, while the conditional probability of packet error P(e/n) only depends on the characteristics of the optical channel.

Single Buffer Deflection Routing

In this section the hop probability distribution P(n) for the two-connected multihop regular topologies MS and SN will be derived under deflection routing in uniform traffic.

Regular topology means that all nodes are topologically equivalent, so that network properties can be deduced by focusing on a single node. Deflection routing [4] is a shortest path routing algorithm where buffer overflow is handled without discarding packets. It is thus a variation on store-and-forward where no packet loss occurs and the queueing delay remains bounded by the number of memory elements provided at each node. The special case where buffers are not provided at all is called hot-potato [3].

In the Manhattan Street Network (Fig. 1a) the $N = n_{MS}^2$ nodes, where n_{MS} is an even integer, are organized in a toroidal grid of n_{MS} rows and n_{MS} columns, with alternating directions like the one-way streets in Manhattan [6]. ShuffleNet (Fig. 1b) is another regular topology in which the $N = n_{SN} 2^{n_{SN}}$ nodes are organized in n_{SN} columns of $2^{n_{SN}}$ nodes each, and each column is connected to the next column in perfect shuffle [7].

There are three structural properties whose interplay determines the performance of a multihop network under deflection routing. The *diameter* of the network is the maximum distance in number of hops between any pair of nodes along a shortest path connecting them over all node pairs in the network. The *deflection cost* is the maximum increase in path length due to a single deflection. The *do not care percentage* is the fraction of do not care nodes in the network: for a given destination node any other node in the network is *do not care* if both its output links like on a shortest path to destination.

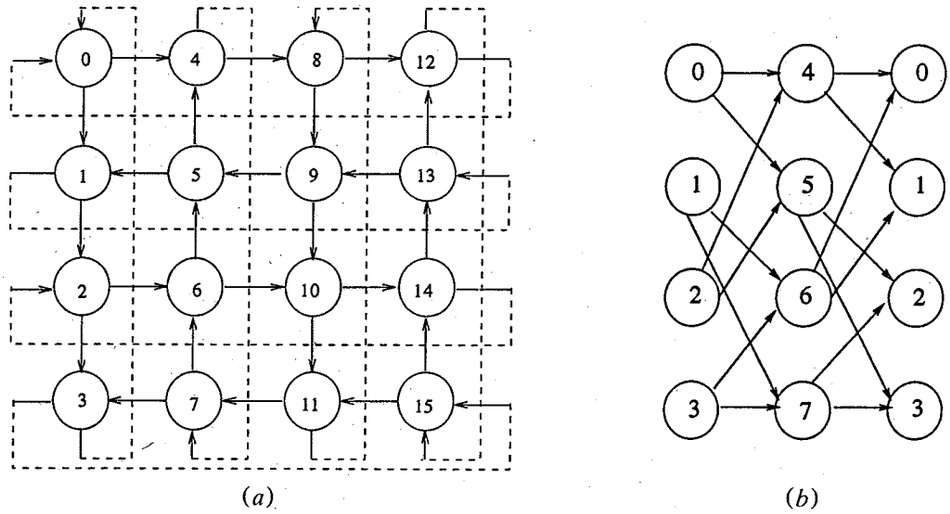

Figure 1. (a) 16-node Manhattan Street Network and (b) 8-node ShuffleNet.

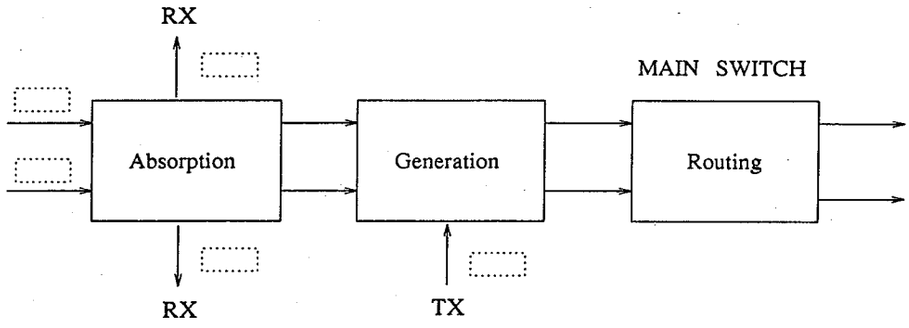

Figure 2. Logical node structure.

A fair comparison between MS and SN is difficult since they exist for distinct sets of number of nodes N whose intersection contains only a few elements. However, many networks with a number of nodes close to within less than 10% can be found and compared. SN has a much lower diameter than MS, and the gap increases with $\sqrt{N}$. The reverse is true for the deflection cost, which is equal to 4 for MS of any size, while it increases as log N for SN. Finally, as N increases, the do not care percentage tends to 0.5 in MS, while it tends to 1 in SN. As it will be shown in the following, SN has a lower average number of hops and hence a higher throughput than MS due to its smaller diameter and higher do not care percentage. The tails of the P(n) distribution are lower in MS due to the lower cost of each deflection.

In the analyzed two-connected networks, the nodes are connected by dedicated fiber links. Slotted transmission with fixed-length packets will be considered.

The logical node structure is shown in Fig. 2. A locally generated packet will be transmitted only if at least one input is free. The structure of the main switch is determined by the specific routing algorithm. With hot-potato routing the main switch is a simple cross-bar switch like the local switches. Some optical buffers can be added to implement buffered deflection routing. A simple scheme to implement all-optical limited-time buffers using fiber delays has been proposed in [8]. Figure 3 shows the structure of the main switch that implements that scheme for a single-buffer memory. S1 and S2 are two cross-bar switches whose state is controlled by a control unit, and the memory element M is a one-slot fiber delay line. This implements a simplified version of a shared output memory since both inputs can access the buffer M through switch S1 and the buffer can access either output through switch S2. A complete structure would need an extra switch to access the memory loop, but this addition does not boost performance significantly, as it will be shown later.

The simplified structure has several attractive features. Optical amplification is not necessary since packets are stored for one time slot only, and the power loss experienced by buffered and unbuffered packets is the same, which helps to keep a small dynamic range at the receiver. Furthermore, a simplified control scheme is possible for very high bit rate applications, in which empty and do not care packets are handled the same way and buffered packets are given priority at the switch S2 [9].

At steady state, these networks can be analyzed by using the one packet model proposed in [10]. A destination is fixed and the trajectory of a test packet with that

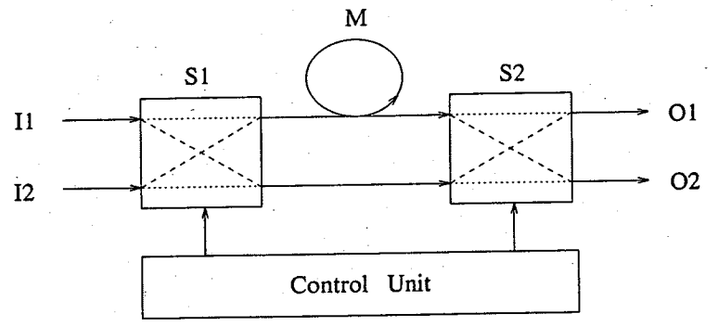

Figure 3. Optical implementation of the routing block with memory. M is the fiber delay line memory, and S1, S2 are cross-bar switches.

destination, randomly generated with uniform probability among all other nodes, is followed. In uniform traffic the trajectory of the test packet can be modeled as a random walk in an isotropic gas of packets. At every care node the test packet can be deflected with probability p. The choice of the destination node is arbitrary due to the regularity of the network. As shown in [9], the effect of adding the above described single buffer memory is a dramatic decrease of the deflection probability p with respect to hot-potato, for instance, from 0.16 to 0.05 for 64-node MS and SN at full load.

Figure 4*a* shows the aggregate throughput, i.e., the number of absorbed/injected packets per slot in the network, versus deflection probability p at full load for 64-node MS and SN. Note that the case $p = 0$ corresponds to S&F with infinite buffers. SN displays a higher throughput than MS for every value of p. The throughput is a decreasing function of deflection probability.

Figure 4*b* shows aggregate throughput versus generation probability g, which is the probability of having a packet ready for transmission at each node at each slot, for a 64-node SN and for hot-potato (H-P), the simplified shared output single buffer memory, (sub) and its complete three-switch version (opt). Curves relative to

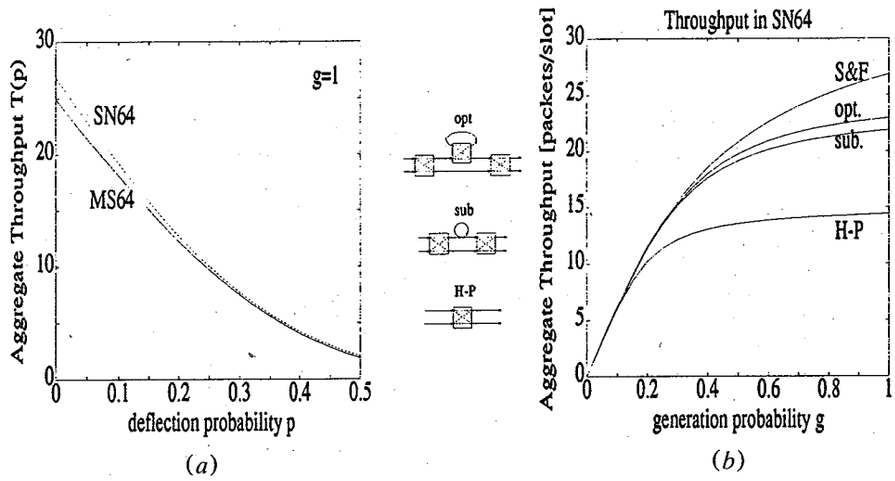

(*a*) (*b*)

Figure 4. (*a*) Aggregate network throughput vs. deflection probability in MS64 and SN64 at full load. (*b*) Aggregate network throughput vs. generation probability in SN64.

S&F with infinite buffers are also given as a reference. One can note the small throughput gain of the three-switch structure with respect to the simplified one. More importantly, it can be noted that the single-buffer memory recovers about 60% of the throughput gap between S&F and hot-potato. Adding more memory elements does not appreciably improve system performance but introduces extra losses and complicates the control algorithm.

The previous figures give the average throughput, which, by Little's theorem [11], is inversely proportional to the average number of hops, i.e., the mean of the P(n) distribution. The probability distribution of the number of hops, however, provides more information than its average value, giving more insight into network behavior. This is important when hop distribution tails must be taken into account for optimizing network performance, such as probability of error, as suggested by Eq. (1). Based on Eq. (1), a comparison between MS and SN in an ultrafast all-optical network will be presented in section four.

Figure 5 shows the hop probability P(n) at full load for MS and SN of comparable size around 400 nodes and their throughput per node. All the P(n) curves decay exponentially with increasing "time" (i.e., number of hops) as it should be in a time-invariant rational linear dynamic system as the one describing the random walk of the test packet. The SN curves are characterized by an initial linear growth and ripples in the tails. In SN, the nodes at a hop distance $j \leq n_{SN}$ to destination are organized in a binary tree structure. Their number thus increases exponentially with j, so the chance that a packet generated from one of those nodes arrives at its destination without being deflected is $(1-p)^j$, and thus the initial linear growth is given by $2^j(1-p)^j/(N-1)$. At distances higher than n_{SN} the number of nodes starts decreasing so that the hop distribution starts decaying. The ripples in the tail have period n_{SN}. This is a consequence of the fact that all deflections have the same cost n_{SN}. In MS the deflection cost is either two or four hops, and ripples with this periodicity are not clearly visible on the given scale.

The key observation is that SN has lower mean, but the tails decay more slowly than in MS, both with and without memory. This behavior reflects the fact that SN

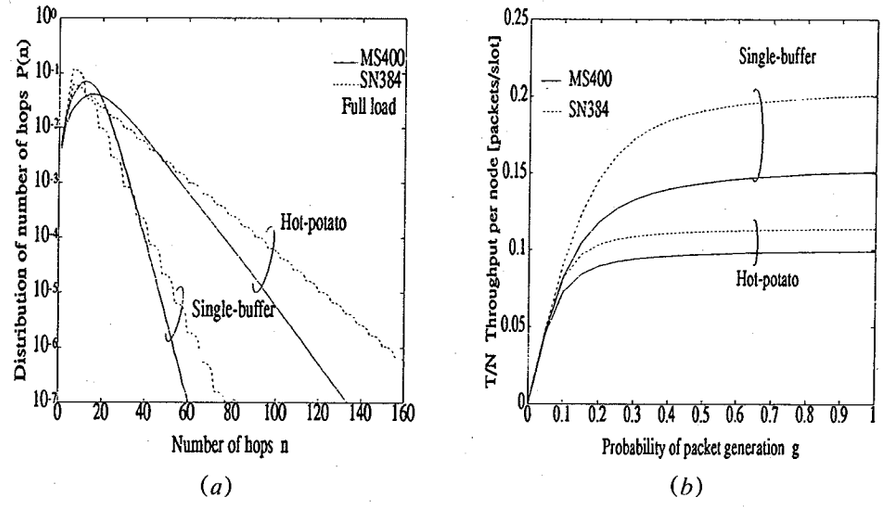

Figure 5. (*a*) Hop probability distribution at full load and (*b*) throughput per node vs. generation probability in MS400 and SN384.

is more compact but has higher deflection cost than MS. In both networks, the tails are dramatically lowered by adding the described single-buffer memory.

These results have been obtained in uniform traffic, where packets are generated at each node with destination chosen at random among all nodes in the network and independently slot by slot. The effect of introducing correlation among the destination of consecutive packets generated at the same node has been investigated by simulation in [9]. It is shown there that the throughput gain obtained with single-buffer deflection routing over hot-potato decreases with the average correlation length since consecutive collisions at the switch saturate the buffer.

Optical Node Structure

The preceding section focused on the structure and the performance analysis of the network from a logical point of view. This section deals with the optical implementation of the main node blocks. Figure 6 shows a block diagram of the optical node structure. Thick lines indicate optical paths, and dashed lines indicate electronic controls. There are two local cross-bar switches SW1 and SW2 for packet reception and transmission and a main switch for packet routing. On each input link a small portion of the incoming signal power is stripped off by an optical coupler and sent to the optoelectronic *header recognition and routing* block. A fiber delay is inserted after the coupler so that incoming packets are sensed before they arrive at the switches, long enough in advance to allow reading the headers, making the routing decisions, and setting the switches. Once a packet's address is recognized to match the node's address, the local switch is set in cross position and the packet is absorbed. At the same time a new packet can be transmitted on the outgoing link.

A key problem in the design of ultrafast, packet-switching networks is the speed matching between the ultrahigh bit rates of the optical channel and the transmitting and receiving electronics. At the receiver, a packet at such ultrahigh rates must be first decompressed by an all-optical demultiplexer and subsequently

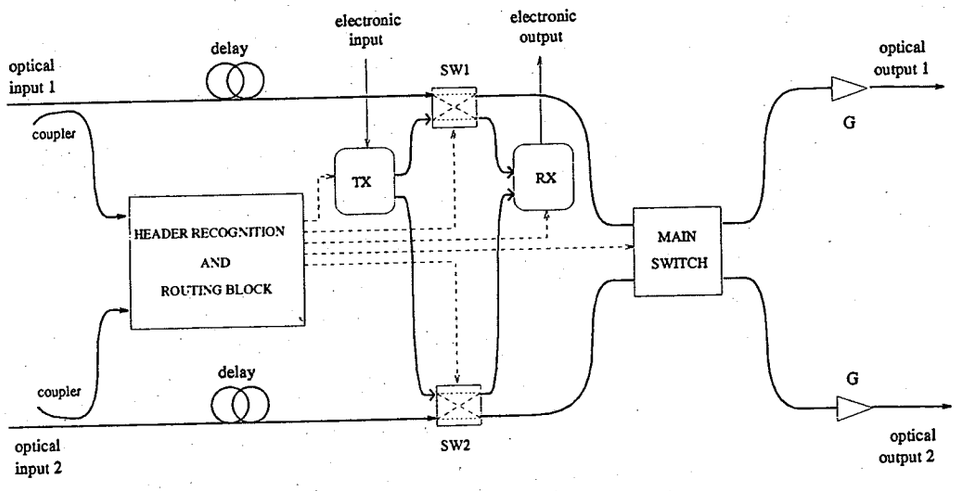

Figure 6. Optical node structure.

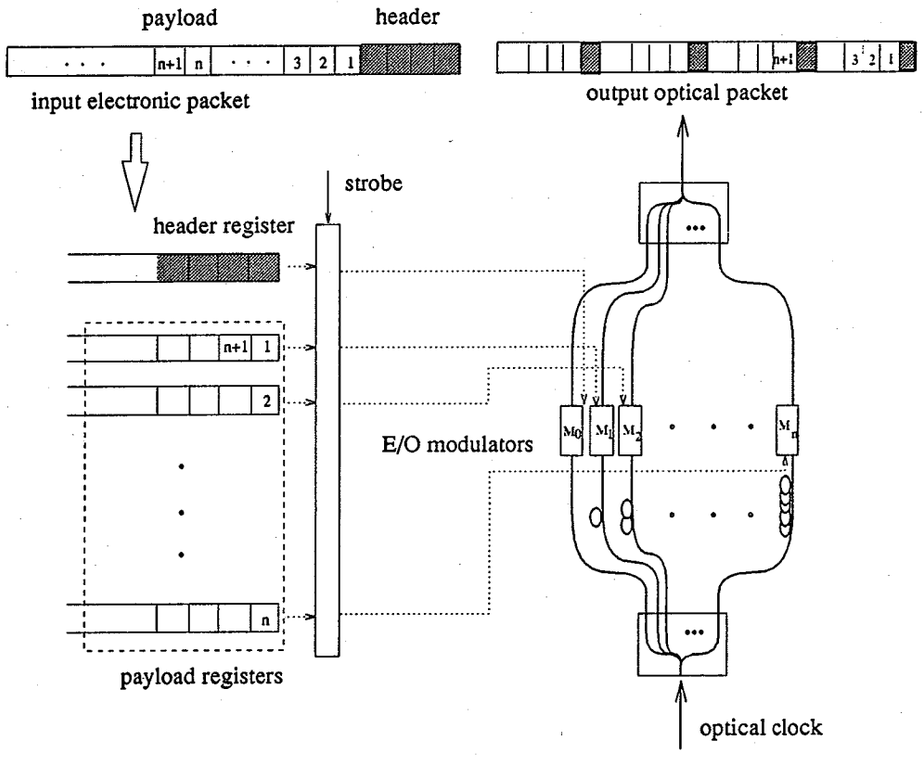

Figure 7. Optical packet generation block.

detected by a parallel bank of conventional optoelectronic detectors. The demultiplexer can be implemented using *all-optical sampling gates*, in which a high-power sampling optical pulse is synchronized on a specific bit position in the packet in order to test whether a pulse is present or not. The sampler works as an optical AND gate, which yields the bit pulse if this is present and no signal otherwise. Several techniques have recently been proposed and demonstrated to implement the all-optical samplers exploiting nonlinear interactions in the fiber [12–14].

The demultiplexer is a $1 \times k$ optical device that de-interleaves the ultrafast input packet at rate R into k optical streams at lower bit rate R/k. With a parallel bank of k optical samplers, packet detection is converted into a parallel detection of extremely short spikes at a repetition rate R/k suitable for electronic detection.

Figure 7 shows the optical packet generation block. The input electronic packet has h header bits and $p = nh$ payload bits, where n is an integer. The header is serially fed into a dedicated shift register. The payload, instead, is fed to a bank of n parallel shift registers. A local optical clock generated by a mode-locked laser produces short optical pulses at a repetition rate $R_c = R/(n + 1)$, where R is the bit rate in the optical packet. The clock output is split into $n + 1$ branches to get one-bit shifted replicas of it, which are fed to an array of $n + 1$ electro-optic modulators. The $n + 1$ shift registers feed the parallel bank of modulators at a modulation rate equal to the clock rate R_c. The modulated optical pulses are recombined into a single stream to yield the optical packet in h clock periods.

With the previous construction, a *spread header* packet structure [15] has been obtained, which allows using only *one* sampling gate for header recognition. The

header, instead of preceding the payload, is spread regularly across the packet in a TDM fashion, as seen in Fig. 7. If the interleaving period between header bits is long enough, the header can be extracted by feeding the packet to a single AND gate together with an optical sampling clock at the interleaving rate and by detecting the output optical signal by an optoelectronic detector.

Figure 8 details the header recognition and routing block. A fraction of the power of the incoming packets is stripped off by a coupler to read the header. A properly delayed version of the same optical clock used for packet generation is optically ANDed with the amplified packet replica to extract the header bits, which are then detected by a fast photodiode and stacked into a fast-access shift register. Based on the contents of the shift register from each input branch, the desired output for each packet is electronically computed and the switch controls are set. These computations can be pipelined to be performed within a packet duration with the fast algorithms available in regular mesh networks [1].

Figure 9 shows the scheme of the receiver. The same technique used to extract the header can be used to demultiplex and detect the payload. One-bit shifted versions of the local sampling clock are sent to an array of n optical sampling gates together with the absorbed packet so that demultiplexing by a factor n is achieved. The n sampled sequences at rate R_c are separately detected by fast photodiodes and electronically buffered. The output of the n electronic shift registers is finally sequentially scanned to obtain parallel-to-serial conversion and yield the received payload at lower electronic rates. The shift registers should have enough buffers to accommodate a stream of back-to-back optical packets and thus match the network's ultrahigh rates to the lower electronic output rates. Amplification might need to be supplied to compensate for the splitting losses of both data and clock, according to the power requirements of the all-optical sampling gates employed.

The advantage of the "spread header" architecture is that only one AND gate is needed in the header recognition block, and the number of demultiplexer branches k can be minimized by using the highest R_c allowed by the processing time of the slowest electronic block in the address recognition and routing pipe. Since with this packet structure the number of clock and packet splittings is minimized, the optical power requirements are also minimized.

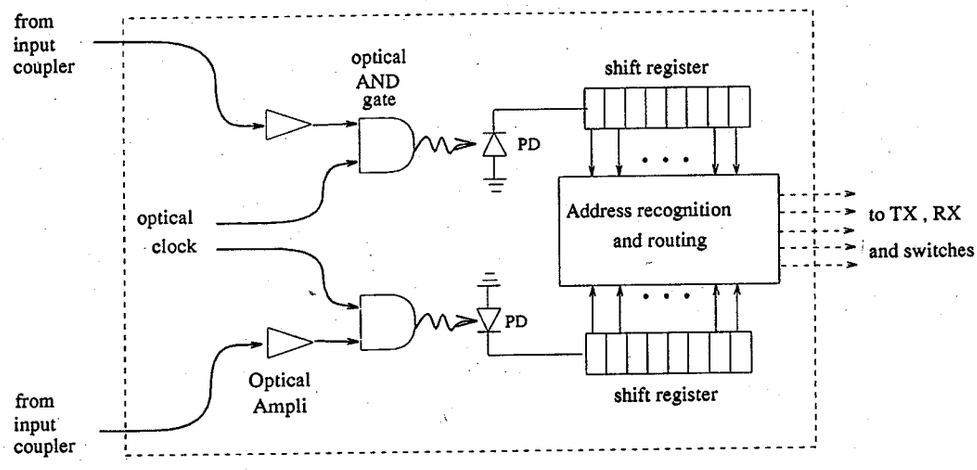

Figure 8. Header recognition and routing block.

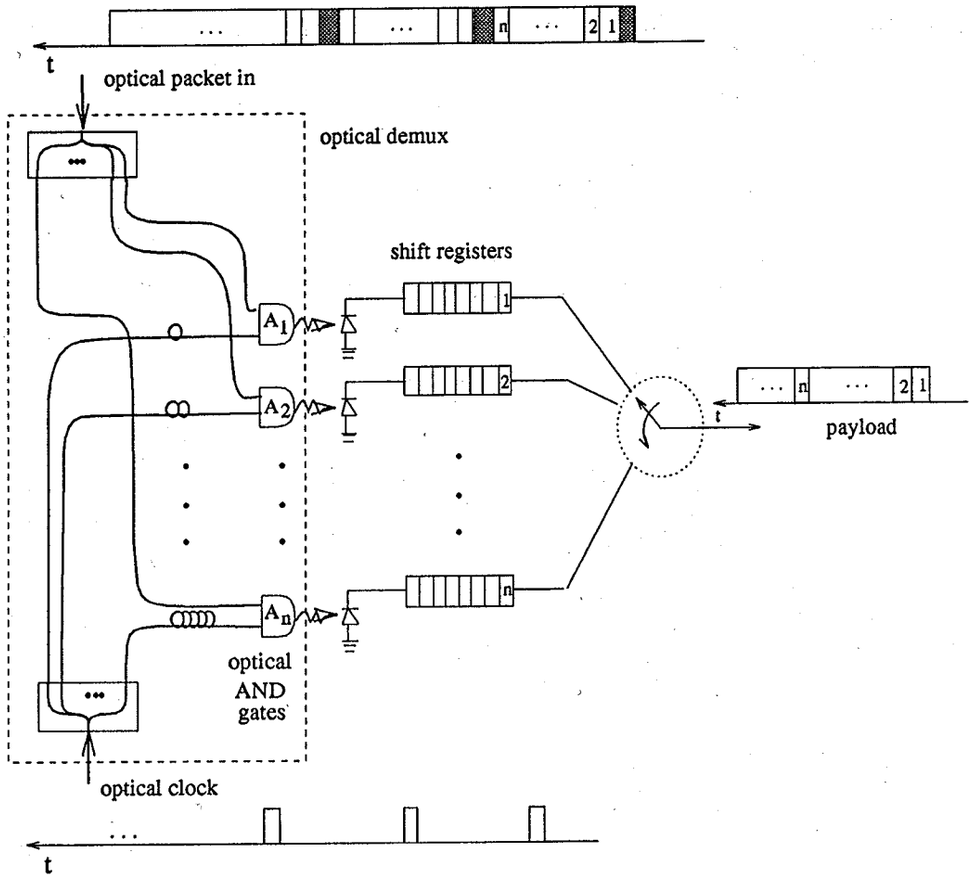

Figure 9. Receiver block diagram.

Channel Limitations in Soliton Networks

In section three, the throughput per node T/N was evaluated by Little's theorem as

$$\frac{T}{N} = \frac{2}{D}u \quad \text{[packets/slot]} \tag{2}$$

where N is the number of nodes; D is the average number of hops, i.e., the mean of P(n); and u is the link occupation probability. However, the throughput in number of bits per second transmitted or received by each node R_{eff}, which is the real parameter of interest, is obtained as

$$R_{\text{eff}} = \frac{2}{D}uR \quad \text{[bit/s]} \tag{3}$$

R_{eff} could in principle be arbitrarily increased by increasing the value of R. However, increasing R has the effect of increasing the error probability at the receiver, so if the packet error rate has to be bounded below a given threshold, R cannot exceed a maximum value, which is a function of network size and load and

of the optical channel. This is clearly seen through Eq. (1), where $P(e)$ is evaluated by conditioning on the number of hops n. The hop distribution $P(n)$ was evaluated in section three. In this section the conditional packet error probability $P(e/n)$ will be derived for the specific case of a soliton channel and the maximum value for R will be found for a threshold value $P(e) = 10^{-6}$.

At ultrahigh bit rates and without regeneration, fiber chromatic dispersion causes strong intersymbol interference. Moreover, high power levels are required to keep a high SNR at the receiver, causing nonlinear distortions of the signal. Solitons have been used in this work because they allow a dynamic compensation between these two effects [16]. Solitons have also been shown to have the highest efficiency of all pulses in the all-optical sampling gates [12], due to their particle-like behavior in switching.

Ideal network synchronization is assumed, i.e., each node knows the nominal arrival time of each bit. Node losses are compensated by lumped optical amplifiers at each node output, while distributed amplification is assumed to compensate for fiber losses. The optical packet receiver is supposed to be a bank of parallel optical sampling AND gates. Each AND gate is modeled as a gating window of width $\tau_w = w\tau$, where τ is the soliton pulsewidth and w the relative window width. The factor w accounts for the sampling time tolerance in the optical sampler. A soliton pulse comes out of the sampling AND gate if its center is inside the corresponding window, and the detected pulse has an energy high enough to justify the assumption that no errors are made when the soliton is inside the sampling window. Errors are caused only by the unpredictable jitter of the pulse position accumulated along the optical path that brings the pulse out of the detection window of the optical AND gate.

Computations are performed by taking into account the jitter due to amplified spontaneous emission noise (ASE) of the optical amplifiers, also known as Gordon-Haus effect [17], soliton self-frequency shift (SSFS) due to Raman scattering, whose effect is inversely proportional to the fourth power of the pulsewidth [18], short-range interaction (SRI) between neighboring solitons [19], and their interplay. At a fixed bit rate, the pulsewidth reduction necessary to avoid short-range interaction strongly enhances the SSFS effect.

The arrival time jitter t_a is therefore the sum of three terms accounting for the above-mentioned effects

$$t_a = t_{SSFS} + t_{ASE} + t_{SRI} \tag{4}$$

t_a can be shown to have conditionally Gaussian statistics that have been evaluated in [20]. Since no error occurs when a "0" (no pulse) is transmitted, nor when a "1" pulse falls inside the window, while an error certainly occurs when a "1" pulse is outside the window, if "0"'s and "1"'s are equally likely, the probability of bit error conditioned on the number of hops n can be obtained as

$$P_b(e/n) + \frac{1}{2}P(\text{pulse out of window}/n) \tag{5}$$

The packet error probability $P(e/n)$ can then be obtained by averaging over the bit pattern. Assuming that each bit in the packet is independently affected, the packet

error rate is from Eq. (1)

$$P(e) = \sum_n \left[1 - [1 - P_b(e/n)]^M\right] P(n) \tag{6}$$

which grows linearly with packet size M when $P(e) \ll 1$.

Figure 10*a* shows the conditional packet error probability for the case of single-buffer deflection routing and for various values of the optical bit rate. Figure 10*b* shows the packet error probability curves, obtained from Eq. (6), plotted versus the optical bit rate R, for MS and SN of 400-node size at full load. These results have been obtained for fiber dispersion parameter $D = 1$ ps/nm/km, for node-to-node distance 1 km, and node amplifier gain per channel $G = 10$ dB for hot-potato and $G = 15$ dB for single-buffer deflection routing, as an extra switch must be added. The packet error probability roughly corresponds to the integral of the hop distribution tails. Since the tails of the hop probability distribution are much higher in SN than in MS, MS allows higher bit rates than SN for low error probability.

The values of R that give $P(e) = 10^{-6}$ have been substituted in Eq. (3) to obtain the curves of throughput R_{eff} in Gb/s, as shown in Fig. 11*a*. This can be compared with the throughput in packets/slot obtained from Eq. (2) for the same networks, as shown in Fig. 5*b*. Under hot-potato routing MS has a slightly higher R_{eff} than SN because of the higher allowed bit rates. However, when single-buffer deflection routing is employed, the tails of the hop distribution get drastically lowered, and even though the allowed bit rate remains higher in MS than in SN, the greater compactness of SN emerges, allowing a higher throughput. Moreover, note that adding the simple single-buffer described in Fig. 3 in a SN384 allows a threefold increase in R_{eff}. The reason is that the buffer has the effect of lowering the delay D, therefore increasing the throughput in packets/slot as seen in Fig. 5*b*, and at the same time allowing higher optical bit rates R, for a given packet error rate, as seen in Fig. 10*b*. These observations show that the choice of the best

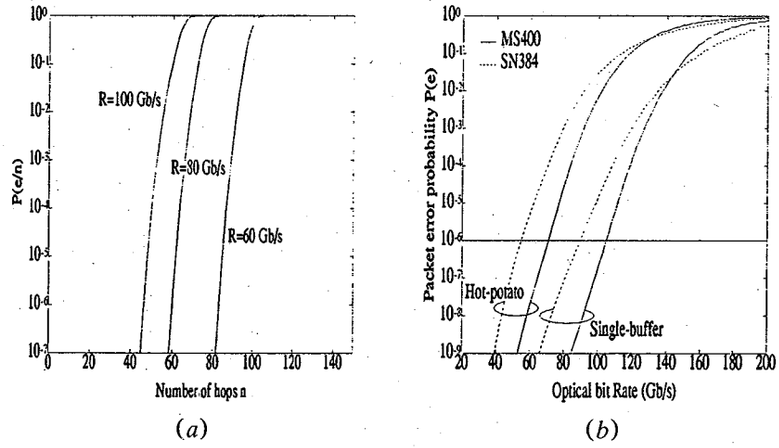

(*a*) (*b*)

Figure 10. (*a*) Conditional packet error probability vs. number of hops for link length 1 km, amplifier gain 15 dB, and bit rate 60, 80, and 100 Gb/s. (*b*) Packet error probability vs. optical bit rate for MS400 and SN384 and 1-km link length.

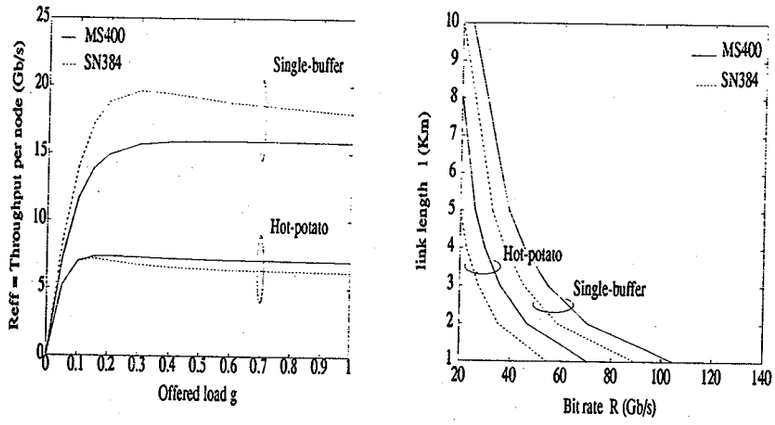

Figure 11. (*a*) Maximum throughput per node to achieve $P(e) \leq 10^{-6}$ vs. offered load in MS400 and SN384 with 1-km link length. (*b*) Maximum optical bit rate to achieve $P(e) \leq 10^{-6}$ vs. link length, at full load.

topology for ultrafast transparent optical networks critically depends on the routing strategy and on the nonlinear optical channel.

The effect of varying the link length has also been addressed. Figure 11*b* shows the maximum node-to-node fiber span l to achieve an error rate $P(e) = 10^{-6}$ as the optical bit rate is increased from 20 to 140 Gb/s. These curves clearly show a "threshold" effect due to an increase in the transmission speed. To keep a constant packet error rate $P(e) = 10^{-6}$, the node-to-node fiber span has to be reduced to a few kilometers as the bit rate R approaches 100 Gb/s. This means that ultrafast all-optical networks without regeneration at bit rates around 100 Gb/s could only be conceived for local or metropolitan area networks, that is, for a physical diameter of the network up to several tens of kilometers, for network sizes up to about 400 nodes.

Dual-wavelength Self-clocking Optical TDMA Broadcast Network

Fiber-optic time division multiple access (FO-TDMA) is attractive for fixed data-rate services and continuous-type traffic, as is the case for high-definition TV (HDTV) broadcasting. A very large number of high bit rate channels can be made available by using ultrashort optical pulses and thereby exploiting the large bandwidth of the optical fiber. Since TDMA is a synchronous scheme, a common time reference is necessary to all the users to guarantee the correct multiplexing. This can be achieved by synchronizing all the transmitters to a common clock source. Naturally the receivers must be able to extract the desired channel by using optical demultiplexers that should be not too complex. The self-clocking technique for bit synchronization presented in this section, due to its simplicity, is particularly suited to implement future low-cost all-optical receivers.

A broadcasting network can be implemented with a tree topology. All the optical transmitters are located in a central office, and the signals are multiplexed and distributed through a cascade of $1 \times n$ optical splitters.

TDMA with transmitter-fixed assignment is assumed; therefore, the receivers shall use tunable optical demultiplexers to extract the desired channel. If ultrashort pulses are used, a specific channel can be extracted at the receiver by logically ANDing its bits with a synchronized version of an optical clock stream. Since extremely low width pulses are involved, synchronization problems arise.

Bit synchronization can be achieved by using an optical phase locked loop (PLL) for timing recovery [21, 22]. However, since the specific application requires low hardware complexity optical PLLs should be avoided.

An alternative approach to bit synchronization is presented here, based on a self-clocking technique [23]. In the proposed scheme a clock stream is transmitted together with the data at a different wavelength [24]. By doing this a wavelength demultiplexer or an optical filter are sufficient in the receiver to recover the clock without the need of an optical PLL.

The block diagram of the proposed network is shown in Fig. 12.

At the transmitting end two mode-locked lasers generate sequences of ultrashort pulses with the same repetition rate at the wavelengths λ_1 and λ_2, synchronized by a common radio-frequency reference.

The first sequence (λ_1) is distributed to the optical transmitters that use their data to gate the laser pulses by means of electro-optic on–off modulators. Each modulated stream is then delayed to the assigned slot and multiplexed with the others through an optical star coupler. To build a frame with correct pulse positioning the fiber length from the lasers to the star coupler must be properly adjusted.

The second sequence (λ_2) is used as a clock signal and is distributed to all the receivers that use it for signal demultiplexing. The clock pulses are accommodated in the first slot of the frame.

In the receiver the desired channel is extracted from the multiplexed stream as follows.

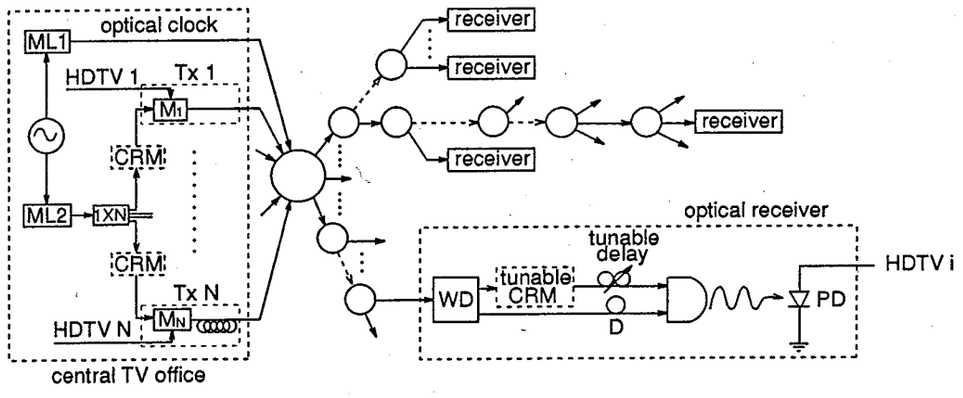

ML: mode-locked laser
M: E/O modulator
WD: wavelength demultiplexer
CRM: clock rate multiplier (present only in the multi-rate case)
PD: photodetector
D: dispersion compensating delay line
Tx: optical transmitter

Figure 12. HDTV distribution based on the proposed dual wavelength TDMA network.

The clock is separated by the data stream by means of a wavelength division demultiplexer or an optical filter. Since the speed of light is different for the two wavelengths, a fiber delay line shall be used to recover the time alignment between clock and data.

The clock signal is then delayed to the desired time slot by using a tunable optical delay line [25], and the delayed clock is sent to an all-optical sampling gate together with the data stream. As mentioned in section four, the sampler works as an optical AND gate that yields the bit pulse when this is present and no signal otherwise. The pulse at the output of the AND gate is then sent to a photodiode to be electronically detected. Since the optically demultiplexed data usually have a pulsewidth much narrower than the pulse interval and are isolated, i.e., data from other channels are not present, a relatively low-speed photodetector and an electronic threshold detector can be used.

One of the possible techniques to realize the AND gate is the nonlinear loop mirror [26]. Since it requires two wavelengths for signal and control (clock), it fits well the proposed dual-wavelength scheme. A power level sufficient to induce the nonlinear switching effect can be obtained by using erbium-doped fiber amplifiers.

The dual-wavelength method for clock distribution is very robust against changes of the fiber length. As explained above, perfect alignment of clock and data is obtained in the receiver by using a fixed delay line whose length depends on the distance between transmitter and receiver and on the wavelengths used. Any variations of the fiber length cause a time misalignment that can be tolerated if it is much less than the pulse width. With extremely short pulses as needed in ultrafast networks, it must be verified that small changes due to mechanical stress or temperature variations do not cause intolerable time misalignment. In the proposed scheme clock and data travel most of the path in the same fiber as the time misalignment Δt is caused only by a variation Δl of the length of that fiber and is given by $\Delta t = D(\lambda_1 - \lambda_2)\,\Delta l$, where D is the fiber chromatic dispersion. Given a typical fiber thermal expansion coefficient of $10^{-6}\mathrm{C}^{-1}$, and a fiber length of 100 km, for 10°C of thermal variation the length variation is $\Delta l = 1$ m. Even with conventional (non-dispersion-shifted) fiber that has typically $D = 15$ ps/nm/km and with wavelength separation of clock and signal of 10 nm the resulting time misalignment is $\Delta t = 0.15$ ps. This robustness facilitates network installation, maintenance and receiver's manufacturing.

A Multi-rate Fiber-optic TDMA Network

This section presents a new ultrahigh-speed fiber-optic TDMA network that can support multirate data communications. A simple method to perform bit synchronization in the proposed multirate network is also introduced, by extending the self-clocking technique discussed in the previous section.

At present, FO-TDMA networks are usually designed with all the users operating at the same data-rate, and this limits their applications. For example, Synchronous Transfer Mode multirate networks will be used to carry TV and HDTV channels at 52 Mbit/s and 156 Mbit/s, respectively, [27] or to support future 150 Mbit/s and 600 Mbit/s broadband communication services. In order to support these applications, FO-TDMA networks should have the ability to offer multirate data communications.

Time-domain multiplexing of N channels with different data rates $f_i = n_i f_0$, integer multiples of f_0, the lowest users' data rate, can be achieved by assigning n_i equally spaced time slots to the ith user in each frame. The total number of time slots in a frame M then has to be chosen as an integer multiple of all the n_i, greater or equal to their sum.

Given N, M, and all the f_i's, satisfying the above constraints, several possible slot assignments can be found by computer search. To improve efficiency in the computer search, higher data-rate channels should be allocated first because their allocation is easier in an "empty" frame. An example of possible time-slot assignment with $M = 24$ is shown in Fig. 13. An efficiency figure for the resulting frame is the ratio between the sum of the required n_i and the frame length M and depends on the particular channel structure to be allocated. For example, when the number of higher-data-rate channels is much lower than the number of basic-rate channels and the difference between high and low data rates is not very large, the scheme is very efficient. In any case, the unassigned slots can be used for adding future channels.

The architecture for the proposed network is the same illustrated in Fig. 12, based on the self-clocking dual-wavelength scheme described in the previous section. The main difference is that clock-rate multipliers (dashed in the figure) must be employed at the transmitter and at the receiver to allow multirate communications [28]. The clock-rate multiplier used in the receiver has to be tunable to allow access to all the channels.

An nf_0 clock stream can be obtained by inserting $n - 1$ equally spaced pulses between consecutive pulses of an f_0 clock stream. This can be done by using a bank of parallel optical delay lines to generate n replicas of the basic-rate clock, shifted by multiples of $\tau = 1/(nf_0)$ as shown in Fig. 14. A tunable optical clock-rate multiplier can be implemented by inserting in each branch an electro-optic switch to enable the proper n branches if the nf_0 rate is desired [28].

The use of different optical clock-rate multipliers at the transmitting end results in different output powers for the channels. This problem could, for example, be solved by using amplified zero-loss splitters/combiners [29] after each clock-rate multiplier.

Conclusion

Some recent results on all-optical packet-switching and broadcasting networks have been presented.

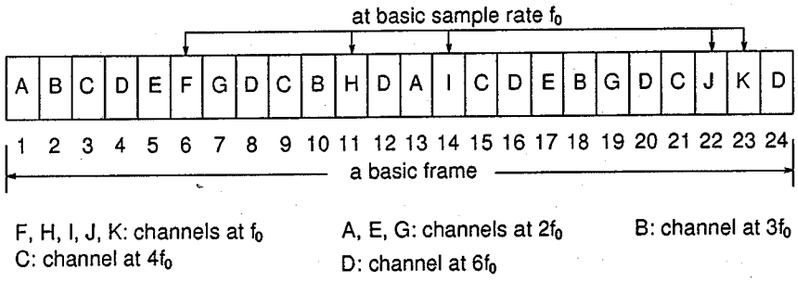

Figure 13. Example of time-slot assignment for a multi-data-rate TDMA frame with $M = 24$.

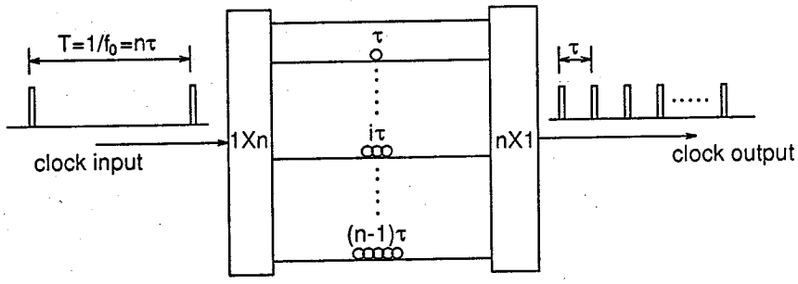

Figure 14. Block diagram of the clock rate multiplier.

The performance evaluation problem of packet-switching transparent optical networks with deflection routing has been addressed for the two-connected Manhattan Street and ShuffleNet network topologies. The effectiveness of a simple single-buffer deflection routing technique has been analytically evaluated and compared to the case of no buffers (hot-potato) and infinite buffers (ideal store-and-forward). For the same networks a theoretical packet error rate analysis has been presented in the case of on–off soliton packet transmission at a fixed optical wavelength and at bit rates in the 100 Gb/s range. It has been shown that, for a given optical bit rate, the size of an all-optical nonregenerative multihop network is limited by the accumulation of noise and distortion in the optical fiber channel.

Novel architectures for all-optical time-domain multiple access broadcast networks have also been considered. In particular, the problem of bit synchronization has been addressed and a new technique, based on the use of two different wavelengths for clock and data, has been proposed. It has been shown how, by using the proposed technique, extremely high aggregate throughput is possible with not too complex optical demultiplexing structures. Finally, an extension of the proposed scheme to the case of multirate data communications has been presented.

All the considered architectures are based on the use of recently proposed all-optical sampling gates to realize the matching of the ultrahigh optical speed allowed by the fiber with the lower speed of the electronic components needed at the user ends. By using such an approach the node structure in the considered all-optical multihop and broadcast networks is greatly simplified.

References

1. N. F. Maxemchuk, "Routing in the Manhattan Street Network," *IEEE Trans. Comm.* **COM-35**, 503–512, May 1987.
2. M. J. Karol and S. Shaikh, "A Simple Adaptive Routing Scheme for ShuffleNet Multihop Lightwave Networks," *Proc. IEEE INFOCOM '88*, paper 50.1, 1640–1647.
3. P. Baran, "On Distributed Communications Networks," *IEEE Trans. Comm. Systems* **12**, 1–9, March 1964.
4. N. F. Maxemchuk, "Regular Mesh Topologies in Local and Metropolitan Area Networks," *AT&T Tech. J.* **64**, 1659–1685, September 1985.
5. A. S. Acampora and A. Shah, "Multihop Lightwave Networks: A Comparison of Store-and-forward and Hot-potato Routing," *IEEE Trans. Comm.* **COM-40**, 1082–1090, June 1992.
6. N. F. Maxemchuk, "The Manhattan Street Network," *Proc. GLOBECOM '85*, 255–261.
7. A. S. Acampora, M. J. Karol, and M. G. Hluchyj, "Terabit Lightwave Networks: The Multihop Approach," *AT&T Tech. J.* **66**, 21–34, November/December 1987.

8. I. Chlamtac and A. Fumagalli, "An All-optical Switch Architecture for Manhattan Networks," *IEEE J. Select. Areas in Comm.*, to appear.
9. F. Forghieri, A. Bononi, and P. R. Prucnal, "Analysis and Comparison of Hot-potato and Single Buffer Deflection Routing in Very High Bit Rate Optical Mesh Networks," *IEEE Trans. Comm.*, to appear.
10. A. G. Greenberg and J. Goodman, "Sharp Approximate Models of Adaptive Routing in Mesh Networks," *Teletraffic Analysis and Computer Performance Evaluation* (O. J. Boxma, J. W. Cohen, and H. C. Tijms, eds.), Elsevier, Amsterdam, 1986, pp. 255–270. "Sharp Approximate Models of Deflection Routing in Mesh Networks," *IEEE Trans. Comm.*, to appear.
11. D. Bertsekas and R. Gallager, *Data Networks*, Prentice-Hall, Englewood Cliffs, NJ, 1987.
12. M. N. Islam, "Ultrafast All-optical Logic Gates Based on Soliton Trapping in Fibers," *Opt. Lett.* **14**, 1257–1259, November 1989.
13. P. A. Andrekson, N. A. Olsson, M. Haner, J. R. Simpson, T. Tanbun-ek, R. A. Logan, D. Coblentz, H. M. Presby, and K. W. Wecht, "32 Gb/s Optical Soliton Data Transmission over 90 km," *IEEE Photon. Technol. Lett.* **4**, 76–79, January 1992.
14. P. A. Andrekson, N. A. Olsson, J. R. Simpson, D. J. Digiovanni, P. A. Morton, T. Tanbun-Ek, R. A. Logan, and K. W. Wecht, "64 Gb/s All-optical Demultiplexing with the Nonlinear Optical-loop Mirror," *IEEE Photon. Technol. Lett.* **4**, 644–647, June 1992.
15. F. Forghieri, A. Bononi, and P. R. Prucnal, "Novel Packet Architecture for All-optical Ultrafast Packet Switching Networks," *Electron. Lett.* **28**, 2289–2291, December 1992.
16. G. P. Agrawal, *Nonlinear Fiber Optics*, Academic Press, New York, 1989.
17. J. P. Gordon and H. A. Haus, "Random Walk of Coherently Amplified Solitons in Optical Fiber Transmission," *Opt. Lett.* **11**, 665–667, October 1986.
18. J. P. Gordon, "Theory of the Soliton Self-frequency Shift," *Opt. Lett.* **11**, 662–664, October 1986.
19. J. P. Gordon, "Interaction Forces Among Solitons in Optical Fibers," *Opt. Lett.* **8**, 596–598, November 1983.
20. A. Bononi, F. Forghieri, and P. R. Prucnal, "Design and Channel Constraint Analysis of Ultra-fast Multihop All-optical Packet Switching Networks with Deflection Routing Employing Solitons," *J. Lightwave Technol.*, submitted.
21. S. Kawanishi and M. Saruwatari, "10 GHz Timing Extraction from Randomly Modulated Optical Pulses Using Phase-locked Loop with Traveling-wave Laser-diode Optical Amplifier Using Optical Gain Modulation," *Electron. Lett.* **28**, 510–512, 1992.
22. K. Smith and J. K. Lucek, "All-optical Clock Recovery Using a Mode-locked Laser," *Electron. Lett.* **28**, 1814–1816, 1992.
23. P. A. Perrier and P. R. Prucnal, "Self-clocked Optical Control of a Self-routed Photonic Switch," *IEEE J. Lightwave Technol.* **7**, 983–989, June 1989.
24. J.-G. Zhang, "Development of High-speed Fiber Optic Networks for Real-time Multimedia Communications," *Proc. SPIE OE/FIBERS '92* **1786**, 11–22, 1992.
25. P. R. Prucnal, M. K. Krol, and J. L. Stacy, "Demonstration of a Rapidly Tunable Optical Time-division Multiple-access Coder," *IEEE Photon. Technol. Lett.*, **3**, 170–172, February 1991.
26. B. P. Nelson, K. J. Blow, P. D. Constantine, N. J. Doran, J. K. Lucek, I. W. Marshall, and K. Smith, "All-optical Gbit/s Switching Using Nonlinear Optical Loop Mirror," *Electron. Lett.* **27**, 704–705, April 1991.
27. S. Kikuchi, N. Yamanaka, and Y. Shimazu, "Optical Wavelength-divison Multiplexing High-speed Switching System for B-ISDN," *Proc. IEEE GLOBECOM '91*, 1235–1239, 1991.
28. J.-G. Zhang, Ph.D. thesis, Dip. di Ingegneria dell'Informazione, Università di Parma, in preparation.
29. H. M. Presby and C. R. Giles, "Amplified Integrated Star Couplers with Zero Loss," *IEEE Photon. Technol. Lett.* **3**, 724–726, August 1991.